

# XIII

## Hadron spectroscopy

Studies of hadron masses, and of both strong and electromagnetic decays of hadrons, provide insights regarding *QCD* dynamics over a variety of distance scales. Among various possible theoretical approaches, the potential model has most heavily been employed in this area. We shall start our discussion by considering heavy-quark bound states, which begin to approximate truly nonrelativistic systems and for which the potential model is expected to provide a suitable basis for discussion.

### XIII-1 The charmonium and bottomonium systems

*Quarkonium* is the bound state of a heavy quark  $Q$  with its antiparticle. Two such systems, charmonium ( $c\bar{c}$ ) and bottomonium ( $b\bar{b}$ ) have been the subject of much experimental and theoretical study; a comprehensive overview is provided by [Br *et al.* 11]. Due to weak decay of the top quark, the  $t\bar{t}$  system has rather different properties from these, and thus constitutes a special case (cf. Sect. XIV-2).

Since the quarkonium systems are quark-antiquark composites, we shall employ the set of quantum numbers  $n, L, S, J$  introduced in Sect. XI-2. One generally refers to the individual quarkonium levels with the nomenclature of Table XIII-1,

Table XIII-1. *Nomenclature for S-wave and P-wave states in the  $c\bar{c}$  and  $b\bar{b}$  systems.*

$L$	$S$	Charmonium	Bottomonium
0	1	$\psi(nS)^a$	$\Upsilon(nS)$
	0	$\eta_c(nS)$	$\eta_b(nS)$
1	1	$\chi_{cJ}(nP)$	$\chi_{bJ}(nP)$
	0	$h_c(nP)$	$h_b(nP)$

<sup>a</sup>For historical reasons, the spin-one charmonium ground state is called  $J/\psi$ .

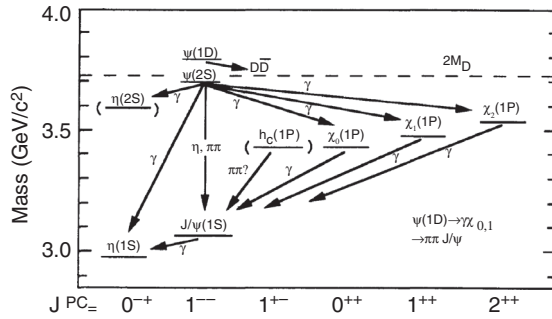


Fig. XIII-1 The low-lying spectrum of charmonium.

although the  $nL$  identification is sometimes replaced by either the degree of excitation or the mass, e.g.,  $\psi(2S)$  is called  $\psi'$  or  $\psi(3686)$ . The  $n^{2S+1}L_J$  spectroscopic notation is also invoked on occasion.

Figs. XIII-1,2 give a summary of the lightest observed  $c\bar{c}$  and  $b\bar{b}$  states. Most of these states, as well as their transitions have been detected both in the charmonium and bottomonium systems [Br *et al.* 11]. The largest set of observed excitations comes from the  $\psi(nS)$  and  $\Upsilon(nS)$  radial towers, reaching up to  $n = 6$  for the  $\Upsilon$  system. Excitation energies are relatively small on the scale of the bottomonium reduced mass  $\mu_b \simeq 2.5$  GeV, but not that of charmonium  $\mu_c \simeq 0.8$  GeV.

*Phenomenological potentials:* Historically, the success of potential models in charmonium was of major importance in convincing the community that quarks were simple dynamical objects and that  $QCD$  provides a manageable theory of the strong interactions. Because of this success, we describe the states by the spectroscopic classification of nonrelativistic quantum mechanics. Thus, quarkonium mass values are often expressed as

$$m_{[nLSJ]} = 2M_Q + E_{[nLSJ]}, \tag{1.1}$$

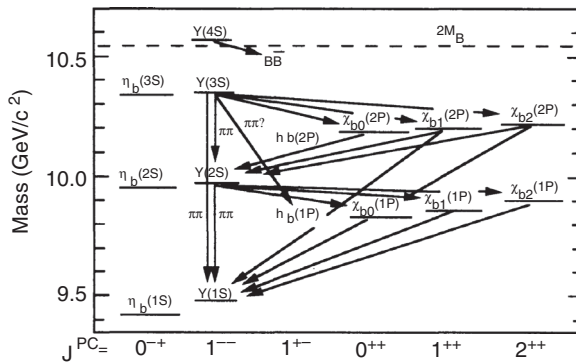


Fig. XIII-2 The low-lying spectrum of bottomonium.

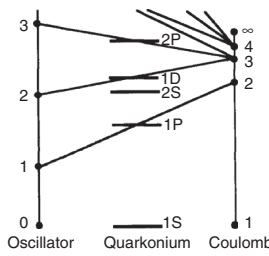


Fig. XIII-3 Energy levels of various potential functions.

where  $E_{[nLSJ]}$  is obtained by solving the Schrodinger equation for a particle of reduced mass  $\mu_Q = M_Q/2$  moving in the field of an assumed potential energy function. The shape of the potential is chosen via a combination of theoretical and phenomenological considerations.

The spectra of quarkonium states already hints at the radial dependence of the  $Q\bar{Q}$  potential, with the progression in  $nL$  levels suggesting an interaction which lies ‘between’ Coulomb and harmonic oscillator potentials, as depicted in Fig. XIII-3. Conceptually, the simplest potential that matches  $QCD$  to this behavior is

$$V(r) = br - \frac{a}{r} + V_0, \tag{1.2}$$

where  $a, b, V_0$  are constants and the color dependence between quark and antiquark is that in Eq. (XI-2.4). The Coulomb-like  $1/r$  component is designed to reproduce one-gluon exchange at short distance. The confining linear ‘ $br$ ’ term models a color-flux tube of constant energy density, as noted in Sect. XI-2. The coefficient  $b$  is commonly described in the literature as the *string tension*, in reference to the string model of hadrons, and its value is estimated from a string model relation involving the typical slope  $\alpha'$  of a hadronic Regge trajectory (cf. Table XIII-2),

$$b = (2\pi\alpha')^{-1} \simeq 0.18 \text{ GeV}^2. \tag{1.3}$$

This is equivalent to a restoring force of about 16 tons!

In practice, phenomenological studies of quarkonium can be carried out by adopting the potential of Eq. (1.2) or another assumed potential energy functions. Examples include the following, e.g.,<sup>1</sup>

$$V(r) = \begin{cases} -\frac{64\pi^2}{27} \mathcal{F} \left\{ \left[ q^2 \ln \left( 1 + (q^2/\Lambda^2) \right) \right]^{-1} \right\} & \{ \Lambda \simeq 0.4 \text{ GeV} \}, \\ br - a/r & \left\{ \begin{array}{l} b \simeq 0.18 \text{ GeV}^2 \\ a \simeq 0.52 \end{array} \right\}, \\ cr^d & \left\{ \begin{array}{l} c \simeq 6.87 \text{ GeV} \\ d \simeq 0.1 \end{array} \right\}, \end{cases} \tag{1.4}$$

<sup>1</sup> The second and third potentials provide fits only up to an additive constant.

Table XIII-2. *Regge trajectories.*

Trajectory	$N$	Slope <sup>a</sup>	$J$ -intercept
$N$	3	0.99	-0.34
$\Delta$	3	0.92	0.07
$\Lambda$	3	0.94	-0.64
$\Sigma$	3	1.1	-1.2
$\Sigma^*$	2	0.91	-0.24
$\pi$	3	0.72	-0.05
$\rho$	4	0.84	0.54
$K$	4	0.69	-0.22
$K^*$	4	0.86	0.29

<sup>a</sup>In units of  $\text{GeV}^{-2}$

where  $\mathcal{F}\{\dots\}$  denotes a Fourier transform. The first two of the potentials in Eq. (1.4) are commonly called the ‘Richardson’ [Ri 79] and ‘Cornell’ [EiGKLY 80] potentials, respectively. They are constructed to mimic  $QCD$  by exhibiting a linear confining potential at long distances and single gluon exchange at short distances. The Richardson potential even incorporates the asymptotic freedom property for the strong interaction coupling. The third is a power-law potential [Ma 81] which, although not motivated by  $QCD$ , can be of use in analytical work or in obtaining simple scaling laws. The power-law potential also serves as a reminder of how alternative forms can achieve a reasonable success in fitting  $b\bar{b}$  and  $c\bar{c}$  spectra, which, after all, are primarily sensitive to the limited length scale  $0.25 \leq r(\text{fm}) \leq 1$ .

From the viewpoint of phenomenology, it is ultimately more useful to appreciate the general features of the  $Q\bar{Q}$  static potential than to dwell on the relative virtues and shortcomings of individual models.

*Effective field theories:* The full theory of  $QCD$  is richer than can be captured in a single potential function. Gluon degrees of freedom can be dynamically active, and field-theoretic corrections introduce subtle modification to masses and couplings. Effective field theory techniques provide a modern way of understanding both the perturbative and nonperturbative properties of heavy-quark systems.

There are various scales associated with quarkonium systems. The heavy-quark mass sets a hard scale. Degrees of freedom associated with this scale may be treated perturbatively. Scales connected to the momentum transfer in the bound state,  $p \sim mv$ , are related to the typical spatial extent,  $\langle r \rangle$ , of the bound state. The time scales involved for quarkonium dynamics are related to the nonrelativistic kinetic energy  $E \sim mv^2/2$ . For large quark mass, the velocity, typically of order

$v^2 \sim 0.1 \rightarrow 0.3$ , can be treated as a small parameter such that each of these scales is technically distinct, with

$$m_Q \gg m_Q v \gg m_Q v^2. \quad (1.5)$$

Different versions of effective field theories can be invoked to treat the different scales [BrPSV 05].

In Non-Relativistic *QCD*, abbreviated as *NRQCD*, degrees of freedom of order  $m_Q$  are integrated out from the theory [CaL 86]. This leaves the light degrees of freedom being the full set of particles of *QCD*. The gluons (and light quarks) are included dynamically, but are treated with an ultraviolet cut-off of order  $m_Q$  because their high-momentum components have been integrated out.<sup>2</sup> The heavy quark itself is treated nonrelativistically. Because the hard modes have been integrated out, there appear higher-order gauge-invariant interactions with Wilson coefficients that parameterize the strength of the new terms. The effective lagrangian then starts out as

$$\mathcal{L} = \mathcal{L}_{0G} + \mathcal{L}_{0Q} + \mathcal{L}_{(\text{h.o.})Q} \quad (1.6)$$

where  $\mathcal{L}_{0G}$  is the usual lagrangian for gluons and  $\mathcal{L}_{0Q}$  is the lowest-order lagrangian for nonrelativistic quarks

$$\mathcal{L}_{0Q} = \psi^\dagger \left[ i D_0 + \frac{C_k}{2m_Q} \mathbf{D}^2 \right] \psi \quad (1.7)$$

where  $D_0$ ,  $\mathbf{D}$  give the coupling of the heavy quarks to gluons. To lowest order in the both the *QCD* coupling constant and in the heavy-quark expansion one can set the Wilson coefficient  $C_k = 1$ , but perturbative corrections lead to different definitions of the heavy-quark mass (see Sect. XIV-1) and  $C_k$  can account for matching onto these definitions. Operators that are higher order in the  $1/m_Q$  expansion also emerge. Examples are

$$\mathcal{L}_{(\text{h.o.})Q} = \psi^\dagger \left[ \frac{C_4}{8m_Q^3} \mathbf{D}^4 + \frac{g_3 C_G}{2m_Q} \boldsymbol{\sigma} \cdot \mathbf{B} \right] \psi + \frac{C_0}{m_Q^2} \psi^\dagger \psi \psi^\dagger \psi + \dots \quad (1.8)$$

The first two terms here describe higher-order interactions with gluons, while the last term is a contact interaction which mimics the effect of a potential. In effective field theory, the contact interaction is appropriate because it comes from the higher-momentum modes above the scale  $p \sim mv$ . The gluonic Coulomb interaction is still treated perturbatively. There will be further contact interactions for different spin and color combinations.

<sup>2</sup> See the discussion of Sec. IV-7.

Because this effective theory includes gluons, there are perturbative corrections also to the heavy-quark mass. These are discussed more fully in Sect. XIV-1. For the purposes here, we will note that the definition of the quark mass is tied up with an overall energy shift in the potential, previously denoted by  $V_0$  in Eq. (1.2). Definitions of the mass which are perturbatively well-behaved are those that are tied to physical thresholds [HoSSW 98]. Effectively, this absorbs  $V_0$  into the definition of the quark mass within some specific prescription. Because this prescription may vary, the appropriate kinetic energy mass in Eq. (1.7) may have a different value, leading to  $C_k \neq 1$ .

One can go further and integrate out degrees of freedom between  $p \sim mv$  and  $E \sim mv^2$ . Since these modes are below the spatial scale of the bound state, contact interactions are no longer appropriate, but they must be replaced by a spatially dependent potential [PiS 98]. Such an effective field theory is labeled  $pNRQCD$ , with the ‘ $p$ ’ referring to the potential. This starts to make closer contact with the phenomenological potential models. However, it remains a field theory and there are controlled perturbative modifications from the so-called ‘*ultra-soft*’ modes which remain dynamical at this scale [HoS 03].

The effective field theory treatments put many of the early successes of phenomenological potential models onto a firmer footing. Moreover, they have also been successful at helping to connect lattice calculations to the phenomenology of quarkonium.

*Lattice studies:* Lattice-gauge theory is well suited to the exploration of the heavy-quark potential [DeD 10, GaL 10, Ro 12]. In the heavy-quark limit, the quarks become static and their interaction energy can be measured by numerical methods. Such studies confirm the general picture of a ‘Coulomb plus linear’ interaction. However, the lattice calculations can also provide the connection between the physical values of the parameters to the underlying scale of  $QCD$ ,  $\Lambda_{QCD}$ .

In general, the static interaction can be described by a function

$$V(r) = - \int \frac{d^3q}{(2\pi)^3} e^{i\mathbf{q}\cdot\mathbf{r}} \frac{a(q^2)}{q^2} \quad (1.9)$$

At large  $q$ , the coefficient  $a(q)$  is determined by the perturbative expansion of  $QCD$ , which has now been accomplished to three-loop order [AnKS 10]. Numerical studies must then match on to the perturbative results at short distance, and this can be accomplished.<sup>3</sup> In doing so, the residual interactions can be mapped onto the operators of  $NRQCD$  and/or the potential of  $pNRQCD$ . While the state of the art continues to advance, the present connection between theory and experiment in the quarkonium spectrum is impressive [Br *et al.* 11].

<sup>3</sup> See, e.g., [Le 98]

### Transitions in quarkonium

All quarkonium states are unstable. Among the decay mechanisms are annihilation processes, hadronic transitions, and radiative transitions. Roughly speaking, the lightest quarkonium states are relatively narrow, but those lying above the *heavy-flavor threshold*, defined as twice the mass of the lightest heavy-flavored meson and depicted by dashed lines in Figs. XIII–1 and XIII–2, are broader. This pattern is particularly apparent for the  $^3S_1$  states – below the heavy-flavor threshold, widths are typically tens of keV, whereas above, they are tens of MeV. The primary reason for this difference is that above the heavy-flavor threshold, quarkonium can rapidly ‘fall apart’ into a pair of heavy-flavored mesons, e.g.,  $\Upsilon[4S] \rightarrow B\bar{B}$ , whereas below, this mode is kinematically forbidden.

In the following, we shall describe only decays which occur beneath the heavy-flavor threshold, and shall limit our discussion to annihilation processes and hadronic decays. Radiative electric and magnetic dipole transitions are adequately described in quantum mechanics textbooks.

*Annihilation transitions:* To motivate a procedure for computing annihilation rates in quarkonium, let us consider the simple case of a charged lepton of mass  $m$  moving nonrelativistically with its antiparticle in a  $^1S_0$  state, and undergoing a transition to a two-photon final state.<sup>4</sup> First, we write down the invariant amplitude for the pair annihilation process,

$$\mathcal{M} = -ie^2\bar{v}(\mathbf{p}_+, \lambda_+) \left[ \not{\epsilon}_2^* \frac{i}{\not{p}_- - \not{q}_1 - m} \not{\epsilon}_1^* + \not{\epsilon}_1^* \frac{i}{\not{p}_- - \not{q}_2 - m} \not{\epsilon}_2^* \right] u(\mathbf{p}_-, \lambda_-), \quad (1.10)$$

for momentum eigenstates. In the lepton rest frame, we are free to choose the *transverse gauge*  $\epsilon_1^* \cdot p_- = \epsilon_2^* \cdot p_- = 0$ , i.e.  $\epsilon_{1,2}^0 = 0$ . Since  $^3S_1$  states can make no contribution to the two-photon mode, we can compute the squared-amplitude for a  $^1S_0$  transition by summing over initial state spins,

$$\sum_{\lambda_{\pm}} |\mathcal{M}|^2 = \frac{e^4}{2m^2} \left[ 2 + \frac{\omega_1}{\omega_2} + \frac{\omega_2}{\omega_1} - 4(\boldsymbol{\epsilon}_1^* \cdot \boldsymbol{\epsilon}_2^*)^2 \right], \quad (1.11)$$

where  $\omega_{1,2}$  are the photon energies in the lepton rest frame. Near threshold, the photons emerge back to back, and the differential cross section is found to be

$$\frac{d\sigma}{d\Omega} = \frac{\alpha^2}{2m^2v_+} \left( 1 - (\boldsymbol{\epsilon}_1^* \cdot \boldsymbol{\epsilon}_2^*)^2 \right). \quad (1.12)$$

Likewise, near threshold, a sum on photon polarizations gives

<sup>4</sup> The  $^1S_0$  ( $^3S_1$ ) states have even (odd) charge conjugation, and can therefore give rise to even (odd) numbers of photons in an annihilation process.

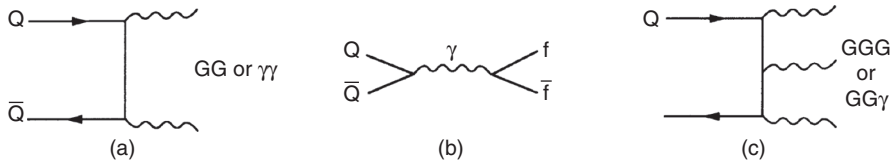


Fig. XIII-4 Decay of quarkonium through annihilation.

$$\sum_{\sigma_{1,2}} \left(1 - (\epsilon_1^* \cdot \epsilon_2^*)^2\right)_{\text{thr}} = 2, \tag{1.13}$$

and upon integrating over half the solid angle (due to photon indistinguishability) we obtain the cross section,

$$\sigma = \frac{4\alpha^2\pi}{m^2 v_+}. \tag{1.14}$$

This is the transition rate per incident flux of antileptons. Since the flux is just the antilepton velocity  $v_+$  times a unit lepton density, we interpret  $v_+\bar{\sigma}$  as the transition rate for a density of *one* lepton per volume. For a bound state with radial quantum number  $n$  and wavefunction  $\Psi_n(\mathbf{x})$ , the density is  $|\Psi_n(0)|^2$  and the lowest-order expression for the electromagnetic decay rate  $\Gamma_{\gamma\gamma}^{(\text{em})}[^1S_0]$  becomes

$$\Gamma_{\gamma\gamma}^{(\text{em})}[^1S_0] = v_+\bar{\sigma}|\Psi_n(0)|^2 = \frac{4\pi\alpha^2}{m^2}|\Psi_n(0)|^2. \tag{1.15}$$

The corresponding rate for  $\gamma\gamma$  emission from  $^1S_0$  states of the  $b\bar{b}$  ( $\Upsilon$ ) system is obtained from Eq. (1.15) by including a factor  $e_b^4 = 1/81$ , which accounts for the  $b$ -quark charge, and a color factor of three. Determination of the two-gluon emission is found similarly (cf. Fig. XIII-4(a)) provided the gluons are taken to be massless free particles, and is left for a problem at the end of the chapter. Including also the effects of  $QCD$  radiative corrections, referred to a common renormalization point  $\mu_R = m_b$ , we have [KwQR 87]

$$\begin{aligned} \Gamma_{\Upsilon \rightarrow \gamma\gamma}[n^1S_0] &= \frac{48\pi\alpha^2|\Psi_n(0)|^2}{81(2m_b)^2} \left[1 - 3.4\frac{\alpha_s(m_b)}{\pi}\right], \\ \Gamma_{\Upsilon \rightarrow gg}[n^1S_0] &= \frac{32\pi\alpha_s^2(m_b)|\Psi_n(0)|^2}{3(2m_b)^2} \left[1 + 4.4\frac{\alpha_s(m_b)}{\pi}\right]. \end{aligned} \tag{1.16}$$

Decays can also occur from the  $n^3S_1$  states.<sup>5</sup> The single-photon intermediate state of Fig. XIII-4(b) leads to emission of a lepton pair, whereas Fig. XIII-4(c) describes final states consisting of three gluons, two gluons and a photon, or three

<sup>5</sup> There are annihilations from higher partial waves as well. These involve derivatives of the wavefunction at the origin.

photons. For such a three-particle final state, there are six Feynman diagrams per amplitude and three-particle phase space to contend with. Upon including  $QCD$  radiative corrections, the results are [KwQR 87]

$$\begin{aligned}
 \Gamma_{\Upsilon \rightarrow \ell \bar{\ell}}[n^3 S_1] &= \frac{16\pi\alpha^2 |\Psi_n(0)|^2}{9(2m_b)^2} \left[ 1 - \frac{16}{3} \frac{\alpha_s(m_b)}{\pi} \right], \\
 \Gamma_{\Upsilon \rightarrow 3g}[n^3 S_1] &= \frac{160(\pi^2 - 9)\alpha_s^3(m_b) |\Psi_n(0)|^2}{81(2m_b)^2} \left[ 1 - 4.9 \frac{\alpha_s(m_b)}{\pi} \right], \\
 \Gamma_{\Upsilon \rightarrow 3\gamma}[n^3 S_1] &= \frac{64(\pi^2 - 9)\alpha^3 |\Psi_n(0)|^2}{2187(2m_b)^2} \left[ 1 - 12.6 \frac{\alpha_s(m_b)}{\pi} \right], \\
 \Gamma_{\Upsilon \rightarrow gg\gamma}[n^3 S_1] &= \frac{128(\pi^2 - 9)\alpha\alpha_s^2(m_b) |\Psi_n(0)|^2}{81(2m_b)^2} \left[ 1 - 1.7 \frac{\alpha_s(m_b)}{\pi} \right]. \quad (1.17)
 \end{aligned}$$

The  $QCD$  contributions in Eq. (1.17) are of interest in several respects. They contribute, on the whole, with rather sizeable coefficients and can substantially affect the annihilation rates. Also, they have come to be used as one of several standard inputs for phenomenological determinations of  $\alpha_s$ . To eliminate the model-dependent factors  $|\Psi_n(0)|^2$ , one works with ratios of annihilation rates,

$$\begin{aligned}
 \frac{\Gamma_{\Upsilon \rightarrow gg\gamma}[n^3 S_1]}{\Gamma_{\Upsilon \rightarrow 3g}[n^3 S_1]} &= \frac{4}{5} \frac{\alpha}{\alpha_s(m_b)} \left( 1 - 2.6 \frac{\alpha_s(m_b)}{\pi} \right), \\
 \frac{\Gamma_{\Upsilon \rightarrow 3g}[n^3 S_1]}{\Gamma_{\Upsilon \rightarrow \mu \bar{\mu}}[n^3 S_1]} &= \frac{10(\pi^2 - 9)\alpha_s^3(m_b)}{9\pi\alpha^2} \left( \frac{M_{\Upsilon}}{2m_b} \right)^2 \left( 1 + 0.43 \frac{\alpha_s(m_b)}{\pi} \right). \quad (1.18)
 \end{aligned}$$

In reality, there are a number of theoretical and experimental concerns which make the extraction of  $\alpha_s(m_b)$  a rather more subtle process than it might at first appear: (i) the contribution of  $|\Psi_n(0)|^2$  in Eqs. (1.16), (1.17) as a strictly multiplicative factor is a consequence of the nonrelativistic approximation and may be affected by relativistic corrections; (ii) there is no assurance that  $\mathcal{O}(\alpha_s)^2$  terms are negligible; particularly in the light of the large first-order corrections; (iii) experiments see not gluons but rather gluon *jets*, and at the mass scale of the upsilon system, jets are not particularly well defined; and (iv) the  $\gamma$  spectrum observed in the  $\gamma gg$  mode is softer than that predicted by perturbative  $QCD$ , implying the presence of important nonperturbative effects. Nevertheless, determinations of this type lead to the central value (and its uncertainties)  $\Lambda_{\overline{MS}}^{(4)} = 296 \pm 10$  MeV as extracted from upsilon data and cited earlier in Table II-2. This example indicates how demanding a task it is to obtain a precise experimental determination of  $\alpha_s(q^2)$ .

*Hadron transitions:* The transitions  $V' \rightarrow V + \pi^0$  and  $V' \rightarrow V + \eta$  involving the decay of an excited  $^3S_1$  quarkonium level ( $V'$ ) down to the  $^3S_1$  ground state ( $V$ ) are interesting because they are forbidden in the limits of flavor- $SU(2)$  and flavor- $SU(3)$  symmetry, respectively. Their rates are therefore governed by quark mass differences, and a ratio of such rates provides a determination of quark mass ratios. There is a modest theoretical subtlety in extracting the rates, as degenerate perturbation theory must be used [IoS 80]. The leading-order effective lagrangian for these  $P$ -wave transitions must be linear in the quark mass matrix  $\mathbf{m}$ ,

$$\begin{aligned} \mathcal{L}_{\text{VVM}} &= -i \frac{c}{2\sqrt{2}} F_\pi \text{Tr} (\mathbf{m} (U - U^\dagger)) \epsilon^{\mu\nu\alpha\beta} \partial_\mu V_\nu \partial_\alpha V'_\beta \\ &= c \left[ (m_d - m_u) \frac{\pi_3}{\sqrt{2}} + (2m_s - m_d - m_u) \frac{\eta_8}{\sqrt{6}} + \dots \right] \epsilon^{\mu\nu\alpha\beta} \partial_\mu V_\nu \partial_\alpha V'_\beta, \end{aligned} \tag{1.19}$$

where  $c$  is a constant. Here,  $\pi_3$  and  $\eta_8$  are the pure  $SU(3)$  states which appear prior to mixing

$$\pi^0 = \cos \theta \pi_3 + \sin \theta \eta_8, \quad \eta = -\sin \theta \pi_3 + \cos \theta \eta_8, \tag{1.20}$$

where  $\tan \theta \simeq \theta = \sqrt{3}(m_d - m_u)/[2(2m_s - m_d - m_u)]$  describes the quark mixing. Upon calculating the transition amplitudes and then substituting for the small mixing angle  $\theta$ , we obtain

$$\begin{aligned} \mathcal{M}_{V' \rightarrow V\pi^0} &= \frac{\mathcal{M}_0}{\sqrt{2}} \left[ m_d - m_u + \frac{2m_s - m_d - m_u}{\sqrt{3}} \theta \right] = \frac{3\mathcal{M}_0}{2\sqrt{2}} (m_d - m_u), \\ \mathcal{M}_{V' \rightarrow V\eta^0} &= \frac{\mathcal{M}_0}{\sqrt{2}} \left[ (m_d - m_u)\theta + \frac{2m_s - m_d - m_u}{\sqrt{3}} \right] \\ &= \frac{2\mathcal{M}_0}{\sqrt{6}} (m_s - \hat{m}) + \mathcal{O} \left( \frac{(m_d - m_u)^2}{m_s} \right), \end{aligned} \tag{1.21}$$

where  $\mathcal{M}_0 \equiv ic \epsilon^{\mu\nu\alpha\beta} k_\mu \epsilon_\nu^* k'_\alpha \epsilon_\beta$ . The ratio of decay rates is found to be

$$\Omega \equiv \frac{\Gamma_{V' \rightarrow V\pi^0}}{\Gamma_{V' \rightarrow V\eta}} = \frac{27}{16} \left| \frac{m_d - m_u}{m_s - \hat{m}} \right|^2 \left| \frac{\mathbf{p}_\pi}{\mathbf{p}_\eta} \right|^3. \tag{1.22}$$

We can extract a quark mass ratio from charmonium data involving  $\psi(2S) \rightarrow J/\psi$  transitions. From the measured value  $\Omega = 0.0396 \pm 0.0033$  [RPP 12], we find

$$\frac{m_d - m_u}{m_s - \hat{m}} = 0.0354 \pm 0.0015, \tag{1.23}$$

which is rather larger than the value in Eq. (VII-1.19) extracted from pion and kaon masses.

### XIII–2 Light mesons and baryons

In the quark model, the light baryons and mesons are  $Q^3$  and  $Q\bar{Q}$  combinations of the  $u, d, s$  quarks. The resulting spectrum is very rich, containing both orbital and radial excitations of the  $L = 0$  ground-state hadrons. For mesons, the  $Q$  and  $\bar{Q}$  spins couple to the total spins  $S = 0, 1$ , and each  $(\mathbf{L}, \mathbf{S})$  combination occurs in the nine flavor configurations of the flavor- $SU(3)$  multiplets  $\mathbf{8}, \mathbf{1}$ . Analogous statements can be made for baryon states.

In the face of such complex spectra, we are mainly interested in the regularities that allow us to extract the essential physics. A tour through the database in [RPP 12] reveals some general patterns.<sup>6</sup> Both radial and orbital excitations of the light hadrons appear  $0.5 \rightarrow 0.7$  GeV above the ground states. As pointed out in Sect. XI–1, this indicates that the light quarks move relativistically. Other striking regularities are (i) the existence of quasi-degenerate *supermultiplets* of particles with differing flavors and equal (or adjoining) spins, and (ii) excitations of a given flavor having increasingly large mass ( $M$ ) and angular momentum ( $J$ ) values, which obey  $J = \alpha' M^2 + J_0$ .

#### *$SU(6)$ classification of the light hadrons*

To the extent that the potential is spin-independent and we work in the limit of equal  $u, d, s$  mass, the quark hamiltonian is invariant under flavor- $SU(3)$  and spin- $SU(2)$  transformations. To lowest order, hadrons are thus placed in irreducible representations of  $SU(6)$ , and quarks are assigned to the fundamental representation  $\mathbf{6}$ ,

$$\mathbf{6} = (u \uparrow \ d \uparrow \ s \uparrow \ u \downarrow \ d \downarrow \ s \downarrow). \quad (2.1)$$

We can also write the  $SU(6)$  quark multiplet in terms of the  $SU(3)$  flavor representation and the spin multiplicity as  $\mathbf{6} = (\mathbf{3}, 2)$ . Although the  $SU(6)$ , invariant limit forms a convenient basis for a classification of the meson and baryon states, it cannot be a full symmetry of Nature since the spin is a spacetime property of particles whereas  $SU(3)$  flavor symmetry is not. Thus, it is impossible to unite the flavor and spin symmetries in a relativistically invariant manner [CoM 67]. Although we shall avoid making detailed predictions based on  $SU(6)$ , it is nonetheless useful in organizing the multitude of observed hadronic levels.

*Meson supermultiplets:* The  $L=0$   $Q\bar{Q}$  composites are contained in the  $SU(6)$  group product  $\mathbf{6} \times \mathbf{6}^* = \mathbf{35} \oplus \mathbf{1}$ , where the representations  $\mathbf{35}, \mathbf{1}$  have flavor–spin content

<sup>6</sup> Our discussion will focus on hadron masses. Strong and electromagnetic transitions are described in [LeOPR 88].

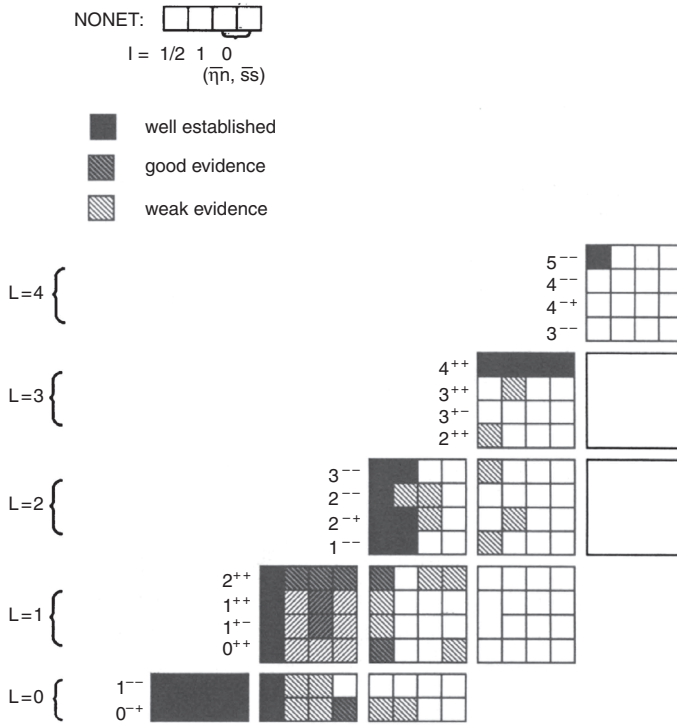


Fig. XIII-5 Spectrum of the light mesons.

$$35 = (8, 3) \oplus (8, 1) \oplus (1, 3), \quad \mathbf{1} = (1, 1). \tag{2.2}$$

The  $L = 0$  ground state consists of a vector octet, a pseudoscalar octet, a vector singlet, and a pseudoscalar singlet. For excited states, the meson supermultiplets constitute an  $SU(6) \times O(3)$  spectrum of particles. The  $O(3)$  label refers to how the total angular momentum is obtained from  $\mathbf{J} = \mathbf{L} + \mathbf{S}$ , giving rise to the pattern of rotational excitations displayed previously in Table XI-3. Roughly speaking, mesons occur in mass bands having a common degree of radial and/or orbital excitation.

Fig. XIII-5 provides a view of the mass spectrum for the lightest mesons. The  $SU(6) \times O(3)$  structure of the ground state and a sequence of orbitally excited states are observed to the extent that sufficient data are available for particle assignments to be made. Note that the  $S$ -wave  $Q\bar{Q}$  states are all accounted for, but gaps appear in all higher partial waves. Even after many years of study, meson phenomenology below 2 GeV is far from complete!

*Baryon supermultiplets:* The  $SU(6)$  baryon multiplet structure arises from the  $Q^3$  group product  $(6 \times 6) \times 6 = (21 \oplus 15) \times 6 = 56 \oplus 70 \oplus 70 \oplus 20$ , and has flavor-spin content

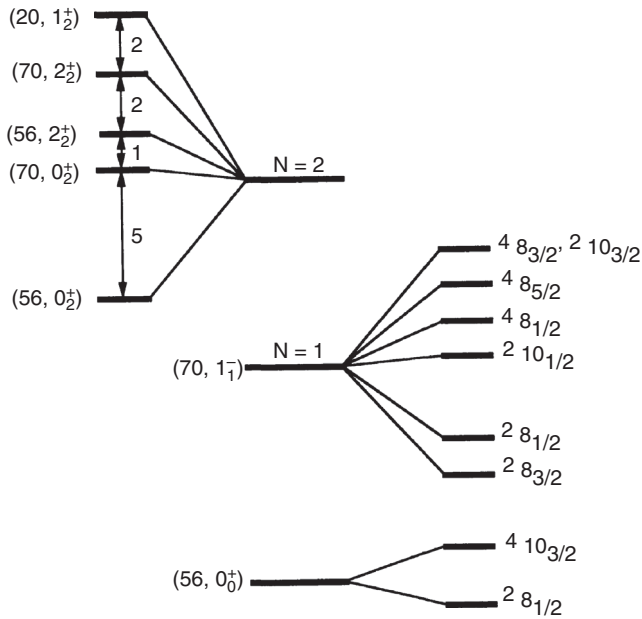


Fig. XIII-6 The low-lying baryon spectrum.

$$\begin{aligned}
 \mathbf{56} &= (\mathbf{10}, 4) \oplus (\mathbf{8}, 2), \\
 \mathbf{70} &= (\mathbf{8}, 4) \oplus (\mathbf{10}, 2) \oplus (\mathbf{8}, 2) \oplus (\mathbf{1}, 2), \\
 \mathbf{20} &= (\mathbf{8}, 2) \oplus (\mathbf{1}, 4).
 \end{aligned}
 \tag{2.3}$$

A three-quark system must adhere to the constraint of Fermi statistics. Each baryon-state vector is thus antisymmetric under the interchange of any two quarks. A Young-tableaux analysis of the above group product reveals that the spin-flavor parts of the **56**, **70** and **20** multiplets are, respectively, symmetric, mixed, and antisymmetric under interchange of pairs of quarks. Since the color part of any  $Q^3$  color-singlet-state vector is antisymmetric under interchange of any two quarks, the **56**-plet has a totally symmetric space wavefunction, with zero orbital angular momentum between each quark pair. The **70** and **20** multiplets require either radial excitations and/or orbital excitations. Recall the characterization of the baryon spectrum in terms of the basis defined by an independent pair of oscillators (cf. Eq. (XI-2.12)). In this context, a standard notation for a baryon supermultiplet is  $(\mathbf{R}, L_N^{\mathcal{P}})$ , where  $\mathbf{R}$  labels the  $SU(6)$  representation,  $\mathcal{P}$  is the parity,  $N$  labels the number of oscillator quanta and  $L$  is the orbital angular momentum quantum number (cf. Sect. XI-2).

Like meson masses, baryon masses tend to cluster in bands having a common value of  $N$ . The first three bands are shown in Fig. XIII-6, and effects of  $SU(6)$  breaking are displayed for the first two. The lowest-lying  $SU(6) \times O(3)$

supermultiplet is the positive-parity ( $\mathbf{56}, 0_0^+$ ), having content as in Eq. (2.3). Next comes the negative-parity ( $\mathbf{70}, 1_1^-$ ) supermultiplet. This contains more states than the  $\mathbf{70}$ -plet shown in Eq. (2.3) because the extension from  $L = 0$  to  $L = 1$  requires addition of angular momenta,

$$\begin{aligned} (\mathbf{10}, 2) &\rightarrow (\mathbf{10}, 4) \oplus (\mathbf{10}, 2), & (\mathbf{8}, 4) &\rightarrow (\mathbf{8}, 6) \oplus (\mathbf{8}, 4) \oplus (\mathbf{8}, 2), \\ (\mathbf{1}, 2) &\rightarrow (\mathbf{1}, 4) \oplus (\mathbf{1}, 2), & (\mathbf{8}, 2) &\rightarrow (\mathbf{8}, 4) \oplus (\mathbf{8}, 2). \end{aligned} \tag{2.4}$$

The number of supermultiplets grows per unit of excitation thereafter. There are five  $SU(6)$  multiplets in the  $N = 2$  band, ( $\mathbf{56}, 2_2^+$ ), ( $\mathbf{56}, 0_2^+$ ), ( $\mathbf{70}, 2_2^+$ ), ( $\mathbf{70}, 0_2^+$ ), and ( $\mathbf{20}, 1_2^+$ ). Recall that the baryonic inter-quark potential was expressed in Eq. (XI-2.10) as  $V = V_{\text{osc}} + U$ , where  $V_{\text{osc}}$  is the potential energy of a harmonic oscillator and  $U \equiv V - V_{\text{osc}}$ . If the potential energy were purely  $V_{\text{osc}}$ , the supermultiplets within the  $N = 2$  band would all be degenerate. In the potential model, assuming that the largest part of  $U$  is purely radial, this degeneracy is removed by the first-order perturbative effect of  $U$ , and the splittings in the  $N = 2$  band are shown at the top of Fig. XIII-6. Aside from choosing the ( $\mathbf{56}, 0_2^+$ ) supermultiplet to have the lowest mass, one finds the pattern of splitting to be as shown in Fig. XIII-6, independent of the particular form of  $U$ .

### Regge trajectories

It is natural to classify together a ground-state hadron and its rotational excitations, e.g., the isospin one-half positive-parity baryons  $N(939)_{J=1/2}$  (the nucleon),  $N(1680)_{J=5/2}$ ,  $N(2220)_{J=9/2}$  and  $N(2700)_{J=13/2}$ . Although no higher-spin entries have been detected in this particular set of nucleonic states (presumably due to experimental limitations), there is no theoretical reason to expect any such sequence to end. The database in [RPP 12] contains a number of similar structures, each characteristically containing three or four members.

Each such collection of states is said to belong to a given *Regge trajectory*. To see how this concept arises, let us consider the simplest case of two spinless particles with scattering amplitude  $f(E, z)$  (i.e.  $d\sigma/d\Omega = |f(E, z)|^2$ ), where  $E$  is the energy and  $z = \cos \theta$  is the scattering angle. It turns out that analytic properties of the scattering amplitude in the complex angular momentum ( $J$ ) plane are of interest. One may obtain a representation of  $f(E, z)$  in the complex  $J$ -plane by converting the partial wave expansion into a so-called *Watson-Sommerfeld transform*,

$$\begin{aligned} f(E, z) &= \sum_{\ell=0}^{\infty} (-)^\ell (2\ell + 1) a(E, \ell) P_\ell(-z) \\ &\rightarrow \frac{1}{2\pi i} \oint_C dJ \frac{\pi}{\sin \pi J} (2J + 1) a(E, J) P_J(-z), \end{aligned} \tag{2.5}$$

where  $P_\ell$  is a Legendre polynomial and  $\mathcal{C}$  is a contour enclosing the nonnegative integers. Suppose that as  $\mathcal{C}$  is deformed away from the  $\text{Re } J$ -axis to, say, a line of constant  $\text{Re } J$ , a pole in the partial wave amplitude  $a(E, J)$  is encountered. Such a singularity is referred to as a *Regge pole* and contributes (cf. Eq. (2.5)) to the full scattering amplitude as

$$f(E, z) = \frac{\beta[E]P_{\alpha[E]}(-z)}{\sin(\pi\alpha[E])} + \dots, \quad (2.6)$$

where  $\alpha[E]$  is the energy-dependent pole position in the complex  $J$ -plane and  $\beta[E]$  is the pole residue.

The Regge-pole contribution of Eq. (2.6) can manifest itself physically in both the direct channel as a resonance and a crossed channel as an exchanged particle. Here, we discuss just the former case by demonstrating how a given Regge pole can be related to a *sequence* of rotational excitations. Suppose that at some energy  $E_R$ , the real part of the pole position equals a nonnegative integer  $\ell$ , i.e.,  $\text{Re } \alpha[E_R] = \ell$ . Then, with the aid of the identity,

$$\frac{1}{2} \int_{-1}^1 dz P_\ell(z) P_\alpha(-z) = \frac{1}{\pi} \frac{\sin(\pi\alpha)}{(\ell - \alpha)(\ell + \alpha + 1)}, \quad (2.7)$$

we can infer from Eq. (2.6) the Breit–Wigner resonance form,

$$a_\ell^{(\text{Rg.-ple.})} = \frac{\beta}{\pi} \frac{1}{(\alpha[E] - \ell)(\alpha[E] + \ell + 1)} \simeq \frac{\Gamma/2}{E - E_R + i\Gamma/2}, \quad (2.8)$$

provided  $\text{Re } \alpha[E_R] \gg \text{Im } \alpha[E_R]$ . A physical resonance thus appears if  $\alpha[E]$  passes near a nonnegative integer and, if the Regge pole moves to ever-increasing  $J$  values in the complex  $J$ -plane as the energy  $E$  is increased, it generates a tower of high-spin states. Except in instances of so-called exchange degeneracy, parity dictates that there be two units of angular momentum between members of a given trajectory. In this manner, a single Regge pole in the angular-momentum plane gives rise to the collection of physical states called a *Regge trajectory*.

A plot of the angular momentum vs. squared-mass for the states on any meson or baryon trajectory reveals the linear behavior,

$$J \simeq \alpha' M^2 + J_0. \quad (2.9)$$

A compilation of slopes ( $\alpha'$ ) and intercepts ( $J_0$ ) appears in Table XIII–2, with each trajectory labeled by its ground-state hadron. Such linearly rising trajectories have been interpreted as a consequence of *QCD* [JoT 76]. In this picture, hadrons undergoing highly excited rotational motion come to approach color-flux tubes, whereupon it becomes possible to relate the angular momentum of rotation to the energy contained in the color field. This line of reasoning leads to the behavior of Eq. (2.9), and accounts for the universality seen in the slope values displayed in Table XIII–2.

***SU(6) breaking effects***

Although an  $SU(6)$ -invariant hamiltonian provides a convenient basis for describing light hadrons, the physical spectrum exhibits substantial departures from the mass degeneracies which occur in this overly symmetric picture. In the following, we shall consider some simple models for explaining the many  $SU(6)$ -breaking effects observed in the real world.

*The QCD Breit–Fermi model:* If one ascribes the nonconfining part of the quark interaction to single-gluon exchange, the nonrelativistic limit yields the ‘QCD Breit–Fermi potential’ [DeGG 75]

$$\begin{aligned}
 V_{\text{one-gluon}} = & -\frac{4k\alpha_s}{3r} \\
 & + \frac{4k\alpha_s}{3} \sum_{i<j} \left[ \frac{8\pi}{3M_i M_j} \mathbf{s}_i \cdot \mathbf{s}_j \delta^3(\mathbf{r}) + \frac{\pi}{2} \delta^3(\mathbf{r}) \left( \frac{1}{M_i^2} + \frac{1}{M_j^2} \right) \right. \\
 & + \frac{1}{M_i M_j r^3} [3(\mathbf{s}_i \cdot \hat{\mathbf{r}})(\mathbf{s}_j \cdot \hat{\mathbf{r}}) - \mathbf{s}_i \cdot \mathbf{s}_j] \\
 & + \frac{1}{r^3} \left( \frac{\mathbf{s}_i \cdot \mathbf{r} \times \mathbf{p}_i}{2M_i^2} - \frac{\mathbf{s}_j \cdot \mathbf{r} \times \mathbf{p}_j}{2M_j^2} - \frac{\mathbf{s}_j \cdot \mathbf{r} \times \mathbf{p}_i - \mathbf{s}_i \cdot \mathbf{r} \times \mathbf{p}_j}{M_i M_j} \right) \\
 & \left. + \frac{1}{2M_i M_j r} (\mathbf{p}_i \cdot \mathbf{p}_j + \hat{\mathbf{r}}(\hat{\mathbf{r}} \cdot \mathbf{p}_i) \cdot \mathbf{p}_j) \right], \quad (2.10)
 \end{aligned}$$

where  $\alpha_s$  is the strong fine structure constant,  $\mathbf{r} \equiv \mathbf{r}_{ij}$ , and  $k$  denotes the color dependence of the potential (cf. Sect. XI-2) with  $k = 1$  (1/2) for mesons (baryons). In keeping with the potential model, the mass parameters  $\{M_i\}$  are interpreted as constituent quark masses. Although the QCD Breit–Fermi model incorporates  $SU(6)$  breaking by means of both quark mass splittings and spin-dependent interactions, it lacks a rigorous theoretical foundation. One might argue on the grounds of asymptotic freedom that Eq. (2.10) does justice to physics at very short distances (in the approximation that  $\alpha_s$  is constant), but there is no reason to believe that it suffices at intermediate-length scales. It also does not account for mixing between isoscalar mesons, so such states must be considered separately.

*Meson masses:* The gluon-exchange model can be used to obtain information on constituent quark mass. In the following, we shall temporarily ignore the minor effect of isospin breaking by working with  $\hat{M} \equiv (M_u + M_d)/2$ . To compute meson masses, we take the expectation value of the full hamiltonian between  $SU(6)$  eigenstates, specifically the  $L = 0$   $Q\bar{Q}$  states.<sup>7</sup> Although the form of Eq. (2.10) implies the presence of spin–spin, spin–orbit, and tensor interactions, the spin–orbit and

<sup>7</sup> An analysis of spin dependence in the  $L = 1$  states is the subject of a problem at the end of the chapter (cf. Prob. XIII-3)).

tensor terms do not contribute here because each quark pair moves in an  $S$  wave, and it is the spin–spin (hyperfine) interaction which lifts the vector meson states relative to the pseudoscalar mesons. We can parameterize the nonisoscalar  $L = 0$  meson masses as

$$m_{Q\bar{Q}}^{(L=0)} = \hat{n}\hat{M} + n_s M_s + \frac{\langle \mathbf{p}_Q^2 \rangle}{2M_Q} + \frac{\langle \mathbf{p}_{\bar{Q}}^2 \rangle}{2M_{\bar{Q}}} + \mathcal{H}_{Q\bar{Q}} \langle \mathbf{s}_Q \cdot \mathbf{s}_{\bar{Q}} \rangle, \quad (2.11)$$

where  $\hat{n}$  and  $n_s$  are the number of nonstrange (n) and strange constituents (s) respectively, and  $\mathcal{H}_{Q\bar{Q}}$  refers to the hyperfine interaction in the second line of Eq. (2.10).

One consequence of Eq. (2.11) is a relation involving the mass ratio  $\hat{M}/M_s$ . Fitting the four masses  $\pi(138)$ ,  $K(496)$ ,  $\rho(770)$ ,  $K^*(892)$  to the parameters in Eq. (2.11) yields

$$\frac{m_{K^*} - m_K}{m_\rho - m_\pi} = \frac{\mathcal{H}_{\text{ns}}}{\mathcal{H}_{\text{nn}}} = \frac{\hat{M}}{M_s} \simeq 0.63. \quad (2.12)$$

The origin of this result lies in the inverse dependence of the hyperfine interaction upon constituent quark mass, which affects the mass splitting between  $S = 1$  and  $S = 0$  mesons differently for strange and nonstrange mesons. The numerical value of  $\hat{M}/M_s$  in Eq. (2.12) graphically demonstrates the difference between constituent quark masses and current quark masses, the latter having a mass ratio of about 0.04. In earlier sections of this book, which stressed the role of chiral symmetry, the pion was given a special status as a quasi-Goldstone particle. In the  $Q\bar{Q}$  model, the small pion mass is seen to be a consequence of severe cancellation between the spin-independent and spin-dependent contributions. However, the parameterization of Eq. (2.11) cannot explain the large  $\eta'(960)$  mass.

In addition to the  $SU(6)$  symmetry-breaking effects of mass and spin, there is an additive contribution present in the isoscalar channel, which is induced by quark–antiquark annihilation into gluons. In the basis of  $u, d, s$  quark flavor states, this annihilation process produces a  $3 \times 3$  mass matrix of the form

$$\begin{pmatrix} 2M_u + X & X & X \\ X & 2M_d + X & X \\ X & X & 2M_s + X \end{pmatrix}, \quad (2.13)$$

where for  $C = +1(-1)$  mesons,  $X$  is the two-gluon (three-gluon) annihilation amplitude, and for simplicity we display just the quark mass contribution ( $2M_i$ ) as the nonmixing mass contribution. The annihilation process is a short-range phenomenon, so the magnitude of  $X$  depends sharply on the orbital angular momentum  $L$  of the  $Q\bar{Q}$  system. For  $L \neq 0$  waves (where the wavefunction vanishes at zero relative separation), and  $C = -1$  channels (where the annihilation amplitude is suppressed by the three powers of gluon coupling), we expect  $M_s - \hat{M} \gg X$ . In this

limit, diagonalization of Eq. (2.13) yields to leading order the set of basis states  $(\bar{u}u \pm \bar{d}d)/\sqrt{2}$  and  $\bar{s}s$ . Only the  $L = 0$  pseudoscalar channel experiences opposite limit  $X \gg M_s - \hat{M}$ , wherein to leading order the basis vectors are the  $SU(3)$  singlet state  $(\bar{u}u + \bar{d}d + \bar{s}s)/\sqrt{3}$  and octet states  $(\bar{u}u - \bar{d}d)/\sqrt{2}$ ,  $(\bar{u}u + \bar{d}d - 2\bar{s}s)/\sqrt{6}$ . The overall picture that emerges is one of relatively unmixed light pseudoscalar states, and heavily mixed vector, tensor, etc., states.

*Baryon masses:* Applying the one-gluon exchange potential to the ground-state baryons of  $(\mathbf{56}, 0_0^+)$  yields a mass formula analogous to Eq. (2.11),

$$m_{Q^3}^{(L=0)} = \hat{n}\hat{M} + n_s M_s + \sum_{i=1}^3 \frac{\langle \mathbf{p}_i^2 \rangle}{2M_i} + \frac{1}{2} \sum_{i<j} \mathcal{H}_{ij} \langle \mathbf{s}_i \cdot \mathbf{s}_j \rangle. \quad (2.14)$$

For the system of  $1/2^+$  and  $3/2^+$  (isospin-averaged) baryons, there are eight mass values and since the above mass formula contains five parameters, one should obtain three relations. The additional perturbative assumption  $\mathcal{H}_{ss} - \mathcal{H}_{ns} = \mathcal{H}_{ns} - \mathcal{H}_{nn}$  for the hyperfine mass parameters yields the Gell-Mann–Okubo relation of Eq. (XII-3.10) for the  $1/2^+$  baryons and the *equal spacing rule* for  $3/2^+$  states,

$$m_{\Sigma^*} - m_{\Delta} = m_{\Xi^*} - m_{\Sigma^*} = m_{\Omega} - m_{\Xi^*}. \\ (\text{Expt. } 153 \text{ MeV} = 149 \text{ MeV} = 139 \text{ MeV}) \quad (2.15)$$

A third relation which relates the  $3/2^+$  and  $1/2^+$  masses and is independent of further perturbative assumptions has the form

$$3m_{\Lambda} - m_{\Sigma} - 2m_N = 2(m_{\Sigma^*} - m_{\Delta}) \\ (\text{Expt. : } 276 \text{ MeV} = 305 \text{ MeV}) \quad (2.16)$$

In addition, one can obtain estimates for  $\hat{M}/M_s$ , among them

$$\frac{\hat{M}}{M_s} = \frac{2(m_{\Sigma^*} - m_{\Sigma})}{2m_{\Sigma^*} + m_{\Sigma} - 3m_{\Lambda}} \simeq 0.62, \\ \frac{\hat{M}}{M_s} = \frac{m_{\Sigma^*} - m_{\Sigma}}{m_{\Delta} - m_N} \simeq 0.65, \quad (2.17)$$

both in accord with Eq. (2.12).

*Isospin-breaking effects:* The above description of  $SU(6)$  breaking assumes isospin conservation. In fact, hadrons exhibit small mass splittings within isospin multiplets, arising from electromagnetism and the  $u - d$  mass difference. In the pion and kaon systems, we were able to use chiral  $SU(3)$  symmetry to isolate each of these separately. Unfortunately, this is not possible in general, and models are required to address this issue.

There are a few consequences which follow purely from symmetry considerations. Since the mass difference  $m_u - m_d$  is  $\Delta I = 1$ , the  $\Delta I = 2$  combinations

$$m_{\Sigma^+} + m_{\Sigma^-} - 2m_{\Sigma^0} = 1.7 \pm 0.1 \text{ MeV}, \quad m_{\rho^+} - m_{\rho^0} = -0.3 \pm 2.2 \text{ MeV}, \quad (2.18)$$

arise only from the electromagnetic interaction. In addition, both electromagnetic and quark mass contributions satisfy the *Coleman–Glashow relation* [CoG 64],

$$m_{\Sigma^+} - m_{\Sigma^-} + m_n - m_p + m_{\Xi^-} - m_{\Xi^0} = 0 \\ [\text{Expt. } 0.4 \pm 0.6 \text{ MeV} = 0]. \quad (2.19)$$

For electromagnetism, this is a consequence of the  $U$ -spin-singlet character of the current, whereas for quark masses it follows from the  $\Delta I = 1$  and  $SU(3)$ -octet character of the current.

We proceed further by using a simple model, based on the  $QED$  Coulomb and hyperfine effects, to describe the electromagnetic interaction of quarks,

$$\Delta m_{\text{coul}} = \mathcal{A}_{\text{coul}} \sum_{i < j} Q_i Q_j, \\ \Delta m_{\text{hyp}} = -\mathcal{A}_{\text{hyp}} \sum_{i < j} \frac{Q_i Q_j}{M_i M_j} \mathbf{s}_i \cdot \mathbf{s}_j, \quad (2.20)$$

where  $\mathcal{A}_{\text{coul}}$ ,  $\mathcal{A}_{\text{hyp}}$  are constants,  $\{Q_i\}$  are quark electric charges, and the sums are taken over constituent quarks. In  $\Delta m_{\text{hyp}}$ , we shall neglect further isospin breaking in the masses and use  $M_u = M_d = \hat{M}$ , and assume electromagnetic self-interactions of a quark to be already accounted for in the mass parameter of that quark. For any values of  $\mathcal{A}_{\text{coul}}$  and  $\mathcal{A}_{\text{hyp}}$ , this model contains the sum rule

$$(m_n - m_p)_{\text{em}} = -\frac{1}{3}(m_{\Sigma^+} + m_{\Sigma^-} - 2m_{\Sigma^0}) = -0.57 \pm 0.03 \text{ MeV}, \quad (2.21)$$

leaving the excess due to the quark mass difference,

$$(m_n - m_p)_{\text{qm}} = \frac{m_u - m_d}{2} \cdot \langle n | \bar{u}u - \bar{d}d | n \rangle - \frac{m_u - m_d}{2} \cdot \langle p | \bar{u}u - \bar{d}d | p \rangle \\ \equiv (m_d - m_u)(d_m + f_m)Z_0 \\ = (m_n - m_p) - (m_n - m_p)_{\text{em}} = 1.86 \pm 0.03 \text{ MeV}, \quad (2.22)$$

where the second line in the above uses the parameterization of hyperon mass splittings given in Eq. (XII–3.9). To the extent that this estimate of quark mass differences is meaningful, one obtains the mass ratio,

$$\frac{m_d - m_u}{m_s - \hat{m}} = \frac{(m_n - m_p)_{\text{qm}}}{m_{\Xi} - m_{\Sigma}} \simeq 0.015, \quad (2.23)$$

to be compared to the chiral-symmetry extraction from meson masses, which yielded 0.023. With further neglect of terms  $\mathcal{O}(\alpha(M_s - \hat{M}))$  in the hyperfine interaction, this exercise can be repeated for vector mesons to yield

$$\begin{aligned} (m_{K^{*0}} - m_{K^{*+}})_{\text{em}} &= -\frac{2}{3}(m_{\rho^+} - m_{\rho^0}) = 0.2 \pm 1.5 \text{ MeV}, \\ (m_{K^{*0}} - m_{K^{*+}})_{\text{qm}} &= (m_{K^{*0}} - m_{K^{*+}}) - (m_{K^{*0}} - m_{K^{*+}})_{\text{em}} \\ &= 6.5 \pm 1.9 \text{ MeV}, \\ \frac{m_d - m_u}{m_s - \hat{m}} &= \frac{m_{K^{*0}} - m_{K^{*+}}}{m_{K^*} - m_{\rho}} = 0.053 \pm 0.016. \end{aligned} \tag{2.24}$$

The additional assumption that the constants  $\mathcal{A}_{\text{coul}}$  and  $\mathcal{A}_{\text{hyp}}$  are the same in the decuplet baryons and the octet baryons, as is true in the  $SU(6)$  limit, leads to

$$\begin{aligned} (m_{\Delta^{++}} - m_{\Delta^0})_{\text{em}} &= \frac{5}{3}(m_{\Sigma^+} + m_{\Sigma^-} - 2m_{\Sigma^0}) = 2.8 \pm 0.2 \text{ MeV}, \\ (m_{\Delta^{++}} - m_{\Delta^0})_{\text{qm}} &= (m_{\Delta^{++}} - m_{\Delta^0}) - (m_{\Delta^{++}} - m_{\Delta^0})_{\text{em}} \\ &= -5.5 \pm 0.4 \text{ MeV}, \\ \frac{m_d - m_u}{m_s - \hat{m}} &= \frac{1}{2} \frac{m_{\Delta^0} - m_{\Delta^{++}}}{m_{\Sigma^*} - m_{\Delta}} = 0.018 \pm 0.002. \end{aligned} \tag{2.25}$$

Of course, the spread of values for the mass ratios raises a concern about the validity of this simple model. However, all methods of calculation agree on the smallness of the ratio  $(m_d - m_u)/(m_s - \hat{m})$ .

### XIII-3 The heavy-quark limit

In the quark description, a heavy-flavored hadron contains at least one of the heavy quarks  $c, b, t$ . An effective field theory, Heavy Quark Effective Theory (HQET), has been developed which provides a powerful tool for heavy quark physics. This involves a study of the limit ( $m_Q \rightarrow \infty$ ) in which the theory is expanded in powers of  $m_Q^{-1}$ . We describe a simple introduction to the topic and much more detail can be found in [MaW 07].

#### *Heavy-flavored hadrons in the quark model*

The spectroscopy of heavy-flavored hadrons should qualitatively follow that of the light hadronic spectrum, with states containing a single heavy-quark  $Q$  occurring as either mesons ( $Q\bar{q}$ ) or baryons ( $Qq_1q_2$ ). The lowest-energy state for a given hadronic flavor will have zero orbital angular momentum between the quarks, leading to ground-state spin values  $S = 0, 1$  for mesons and  $S = 1/2, 3/2$  for

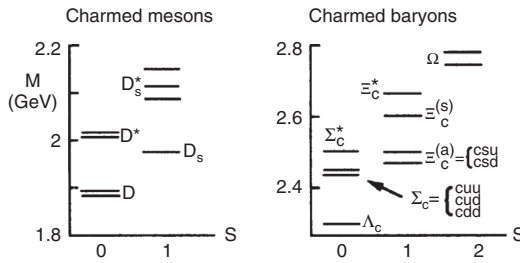


Fig. XIII-7 Spectrum of charmed (a) mesons, (b) baryons.

baryons. The hyperfine interaction will lower the  $S = 0$  meson and  $S = 1/2$  baryon masses, and both orbital and radial hadronic excitations of the ground state will be present.

Although it is possible to contemplate extended flavor transformations which involve interchange of the light and heavy quarks, e.g., as in the  $SU(4)$  of the light and charmed hadrons, such symmetries are so badly broken by the difference in energy scales  $M_Q \gg M_q$  and  $M_Q \gg \Lambda_{QCD}$  as to be rendered useless. The  $SU(3)$ - and  $SU(2)$ -flavor symmetries associated with the light hadrons are still viable, but multiplet patterns become modified. The mesons  $Q\bar{q}$  will exist in the  $SU(3)$  multiplet  $\mathbf{3}^*$ , whereas in the baryonic  $Qq_1q_2$  configurations the two light quarks  $q_1, q_2$  will form the flavor- $SU(3)$  multiplets  $\mathbf{6}$  and  $\mathbf{3}^*$ . For example, the charmed system has the meson ground state

$$\mathbf{3}^* : D^+ [c\bar{d}], D^0 [c\bar{u}], D^s [c\bar{s}],$$

which displays the mass pattern of an  $SU(2)$  doublet ( $D_{1869}^+, D_{1865}^0$ ) and an  $SU(2)$  singlet ( $D_{1969}^s$ ). The charmed-baryon multiplets are

$$\begin{aligned} \mathbf{6} : & \Sigma_c^{++}[uuc], \Sigma_c^+[udc], \Sigma_c^0[ddc], \Xi_c^{+(s)}[usc], \Xi_c^{0(s)}[dsc], \Omega_c^0[ssc] \\ \mathbf{3}^* : & \Lambda_c^+[udc], \Xi_c^{+a}[usc], \Xi_c^{0a}[dsc]. \end{aligned}$$

Fig. XIII-7 displays the anticipated charmed-meson and charmed-baryon levels, including the effect of  $SU(3)$  breaking.

Heavy-quark constituent mass values can be inferred from the  $D^* - D$  and  $B^* - B$  hyperfine splittings. That the former splitting is about three times the latter is a consequence of  $M_b \simeq 3M_c$  and of the inverse dependence of the hyperfine effect upon quark mass. Analogously to Eq. (2.17), we find

$$\frac{\hat{M}}{M_c} = \frac{m_{D^*} - m_D}{m_\rho - m_\pi} \simeq 0.22, \quad \frac{\hat{M}}{M_b} = \frac{m_{B^*} - m_B}{m_\rho - m_\pi} \simeq 0.08, \quad (3.1)$$

where  $\hat{M} \equiv (M_u + M_d)/2$ . These findings depend to some extent on how the fit is done, e.g., with mesons or with baryons, and we leave further study for Prob. XIII-4.

### *Spectroscopy in the $m_Q \rightarrow \infty$ limit*

In a hadron which contains a single heavy quark  $Q$  along with light degrees of freedom, the heavy quark is essentially static. The best analogy is with atoms, where the nucleus can in the first approximation be treated as a static, electrically charged source. Likewise, for heavy hadrons the heavy quark is a static source with color charge, and the light degrees of freedom provide a nonstatic hadronic environment around  $Q$ . This scenario can be formalized by partitioning the heavy-quark lagrangian as [CaL 86, Ei 88, LeT 88]

$$\begin{aligned}\mathcal{L}_Q &= \bar{\psi} (i \not{D} - m_Q) \psi \equiv \mathcal{L}_0 + \mathcal{L}_{\text{space}} \\ \mathcal{L}_0 &= \bar{\psi} (i \gamma_0 D_0 - m_Q) \psi, \quad \mathcal{L}_{\text{space}} = -i \bar{\psi} \boldsymbol{\gamma} \cdot \mathbf{D} \psi,\end{aligned}\quad (3.2)$$

where  $D_\mu \psi$  is the covariant derivative of  $SU(3)_c$ . Since the spatial  $\boldsymbol{\gamma}$  matrices connect upper and lower components, we see that the effect of  $\mathcal{L}_{\text{space}}$  is  $\mathcal{O}(m_Q^{-1})$ .

Observe that the static lagrangian  $\mathcal{L}_0$  of Eq. (3.2) is invariant under spin rotations of the heavy quark  $Q$ . In the world defined by  $\mathcal{L}_0$ , with both  $\mathcal{O}(\Lambda_{QCD}/M_Q)$  effects and  $\mathcal{O}(\alpha_s(M_Q))$  effects (associated with hard-gluon exchange) ignored, heavy-hadronic energy levels and couplings are constrained by the  $SU(2)$  spin symmetry. It is helpful to visualize the situation. A heavy-flavored hadron of spin  $\mathbf{S}$  will contain a static quark  $Q$  having a constant spin vector  $\mathbf{S}_Q$  (with  $S_Q = 1/2$ ) and light degrees of freedom having a constant angular momentum vector  $\mathbf{J}_\ell \equiv \mathbf{S} - \mathbf{S}_Q$ .<sup>8</sup> For a meson of this type, we assume that  $J_\ell$  behaves as it does in the quark model, with  $J_\ell = 1/2$  in the ground state and  $J_\ell = L \pm 1/2$  for  $L > 0$  rotational excitations. From the decoupling of the heavy-quark spin, it follows that *there will be a two-fold degeneracy between mesons having spin values  $S = J_\ell \pm 1/2$* . The meson  $L = 0$  ground state will have  $J_\ell = 1/2$  and thus degenerate states with  $S = 0, 1$ . The  $L = 1$  first rotational excitation with  $J_\ell = 1/2$  will give rise to degenerate  $S = 0, 1$  levels, whereas for  $J_\ell = 3/2$  one obtains degenerate levels having  $S = 1, 2$ . Moreover, the energy differences between different levels should be independent of heavy-quark flavor. Analogous conditions hold for heavy flavored baryons, and hadronic transitions between levels of differing  $L$  can be similarly analyzed.

<sup>8</sup> Although the light degree(s) of freedom in the simple quark model is an antiquark  $\bar{q}$  for mesons and two quarks  $q_1 q_2$  for baryons, the physical (i.e. actual) light degrees of freedom could entail unlimited numbers of gluons and/or quark-antiquark pairs.

Let us explicitly demonstrate that the splitting between the  $J^P = 1^-$  and  $J^P = 0^-$  states of a  $Q\bar{q}$  meson must vanish in the limit of infinite quark mass. We note that the mathematical condition for spin-independence is

$$\left[ H_0, S_3^Q \right] = 0, \tag{3.3}$$

where  $S_3^Q$  is the generator of spin rotations about the 3-axis for quark  $Q$  and  $H_0$  is the hamiltonian obtained from  $\mathcal{L}_0$ . Since the action of  $S_3^Q$  on a  $0^-$  state produces a  $1^-$  state, i.e.,  $|M_{1^-}\rangle = 2S_3^Q|M_{0^-}\rangle$ , we then have

$$H_0|M_{1^-}\rangle = m_{1^-}|M_{1^-}\rangle = 2S_3^QH_0|M_{0^-}\rangle = m_{0^-}|M_{1^-}\rangle, \tag{3.4}$$

implying that  $m_{1^-} - m_{0^-} \rightarrow 0$  as  $m_Q \rightarrow \infty$ .

Another consequence of working in the static limit of  $\mathcal{L}_0$  is that the propagator,  $S_\infty(x, y)$ , of the heavy quark in an external field can be determined exactly. From the defining equations,

$$(i\gamma_0 D_0 - m_Q) S_\infty(x, y) = \delta^{(4)}(x - y) \quad (D_0 \equiv \partial_0 + ig_3\mathbf{A}_0 \cdot \boldsymbol{\lambda}/2), \tag{3.5}$$

one has the solution

$$S_\infty(x, y) = -iP(x_0, y_0)\delta^{(3)}(\mathbf{x} - \mathbf{y}) \left[ \theta(x^0 - y^0)e^{-im_Q(x^0 - y^0)} \left( \frac{1 + \gamma_0}{2} \right) + \theta(y^0 - x^0)e^{im_Q(x^0 - y^0)} \left( \frac{1 - \gamma_0}{2} \right) \right], \tag{3.6}$$

where  $P(x_0, y_0)$  is the path-ordered exponential along the time direction,

$$P(x_0, y_0) \equiv P \exp \left[ i \frac{g_3}{2} \int_{y^0}^{x_0} dt \boldsymbol{\lambda} \cdot \mathbf{A}_0(\mathbf{x}, t) \right]. \tag{3.7}$$

In this approximation, the heavy quark is static at point  $\mathbf{x}$  and the only time-dependence is that of a phase.

This discussion can be generalized to a frame where the heavy quark is moving at a fixed velocity  $\mathbf{v}$ , described by a velocity-four vector  $v^\mu = p^\mu/m_Q$ , with  $v^\mu v_\mu = 1$ . One can define projection operators

$$\Gamma_{v\pm} = \frac{1}{2} (1 \pm \not{v}), \tag{3.8}$$

where  $\Gamma_{v\pm}^2 = \Gamma_{v\pm}$ ,  $\Gamma_{v\pm}\Gamma_{v\mp} = 0$ , and  $\Gamma_{v+} + \Gamma_{v-} = 1$ . The  $\Gamma_{v\pm}$  generalize the usual projection of ‘upper’ and ‘lower’ components into the moving frame. A quark moving with velocity  $\mathbf{v}$  will have the leading description of its wavefunction contained in the ‘upper’ component described by a field  $h_v$  [Ge 90, Wi 91],

$$\Gamma_{v+}\psi \equiv e^{-im_Q v \cdot x} h_v(x), \tag{3.9}$$

where the main dependence on the quark mass has been factored out, and  $h_v$  obviously satisfies  $\Gamma_{v+}h_v = h_v$ . Substituting into the Dirac lagrangian, neglecting lower components, and using  $\Gamma_{v+}\not{D}\Gamma_{v+} = v \cdot D$  yields

$$\mathcal{L}_Q = \bar{\psi} (i \not{D} - m_Q) \psi \simeq \bar{\psi} \Gamma_{v+} (i \not{D} - m_Q) \Gamma_{v+} \psi = \bar{h}_v i v \cdot D h_v, \quad (3.10)$$

which generates the lowest-order equation of motion  $v \cdot D h_v = 0$ . This approximation can be systematically improved by inclusion of a ‘lower’ component for the heavy-quark field [EiH 90, Lu 90, GeGW 90],

$$\Gamma_{v-}\psi \equiv e^{-im_Q v \cdot x} \ell_v(x), \quad (3.11)$$

with  $\Gamma_{v-}\ell_v = \ell_v$ . The equations of motion allow us to solve for  $\ell_v$  by following the sequence of steps,

$$\begin{aligned} 0 &= (i \not{D} - m_Q) \psi = (i \not{D} - m_Q) e^{-im_Q v \cdot x} [h_v + \ell_v] \\ &= e^{-im_Q v \cdot x} (m_Q (\not{v} - 1) + i e^{-im_Q v \cdot x} \not{D}) [h_v + \ell_v] \\ &= e^{-im_Q v \cdot x} [(-2m_Q + i \not{D})\ell_v + i \not{D} h_v], \end{aligned} \quad (3.12)$$

which yields  $\ell_v$  and  $\psi$  as

$$\begin{aligned} \ell_v &= \frac{i}{2m_Q} \not{D} h_v + \mathcal{O}(m_Q^{-2}) \\ \psi &= e^{-im_Q v \cdot x} \left[ 1 + \frac{i}{2m_Q} \not{D} \right] h_v + \mathcal{O}(m_Q^{-2}). \end{aligned} \quad (3.13)$$

Inserting these forms into Eq. (3.10) and using  $\Gamma_{v+}h_v = h_v$  and Eq. (III-3.50) for  $\not{D}\not{D}$  yields

$$\begin{aligned} \mathcal{L}_v^Q &= \bar{h}_v \left[ i \not{D} - \frac{\not{D}\not{D}}{m_Q} - \frac{\not{D}(\not{v} - 1)\not{D}}{4m_Q} \right] h_v \\ &= \bar{h}_v \left[ i v \cdot D - \frac{1}{2m_Q} \left( D_\mu D^\mu + \frac{1}{4} g_3 \lambda^a \sigma^{\mu\nu} F_{\mu\nu}^a \right) - \frac{(v \cdot D)^2}{2m_Q} \right] h_v, \end{aligned} \quad (3.14)$$

which is the desired expansion in terms of the heavy-quark mass. Because the last term in this expression is second order in  $v \cdot D$  and noting that  $v \cdot D h_v = 0$  to lowest order, it will not contribute to matrix elements at order  $1/m_Q$  and can be dropped. The lagrangian of Eq. (3.14) corresponds to a quark moving at fixed velocity. Anti-quark solutions can be constructed with the mass dependence  $e^{+im_Q v \cdot x}$ , with the result

$$\bar{\mathcal{L}}_v^Q = \bar{k}_v \left[ -i v \cdot D - \frac{1}{2m_Q} \left( D_\mu D^\mu + \frac{1}{4} g_3 \lambda^a \sigma^{\mu\nu} F_{\mu\nu}^a \right) - \frac{(v \cdot D)^2}{2m_Q} \right] k_v, \quad (3.15)$$

where the field  $k_v$  satisfies  $\Gamma_{v-k_v} = k_v$ . It is legitimate to neglect the production of heavy  $Q\bar{Q}$  pairs. However, one should superpose the lagrangians for different velocities in a Lorentz-invariant fashion,

$$\mathcal{L} = \int d^4v \delta(v_\mu v^\mu - 1) \theta(v_0) [\mathcal{L}_v^Q + \mathcal{L}_v^{\bar{Q}}] = \int \frac{d^3v}{2v_0} [\mathcal{L}_v^Q + \mathcal{L}_v^{\bar{Q}}]. \quad (3.16)$$

The nature of the approximation at this stage is more of a classical limit rather than a nonrelativistic limit. To be sure, for any given quark one can work in the quark's rest frame, in which case the quark will be nonrelativistic. However, when external currents act on the fields, transitions from one frame to another occur for which  $\Delta\mathbf{v}$  is *not* small. On the other hand, the result can be said to be classical because quantum corrections have not yet been included and these can renormalize the coefficients in  $L_v^{Q\bar{Q}}$ . Also, diagrams involving the exchange of hard gluons can produce nonstatic intermediate states. Such corrections can be accounted for in perturbation theory [Wi 91].

### XIII-4 Nonconventional hadron states

Many suggestions have been made regarding the possibility of hadronic states beyond those predicted by the simple quark model of  $Q\bar{Q}$  and  $Q^3$  configurations. The study of such states is hampered by the fact that we still have very little idea why the quark model works.  $QCD$  at low energy is a strongly interacting field theory, and we would expect a very rich and complicated description of hadronic structure. That the result should be describable in terms of a simple  $Q\bar{Q}$  and  $Q^3$  picture as even a first approximation remains a mystery. Quark models have been popular because they seem to work phenomenologically, not because they are a controlled approximation to  $QCD$ . This weakness becomes all the more evident when one tries to generalize quark model ideas to new areas.

Much of the theoretical work on nonconventional states has involved the concept of a *constituent gluon*  $G$ , analogous to a constituent quark  $Q$ , and we shall cast our discussion with respect to this degree of freedom.<sup>9</sup> It is clear that there should be a cost in energy to excite a constituent gluon. The energy should not be extremely large, else it would be difficult to understand the early onset of scaling in deep-inelastic scattering. However, it cannot be less than the uncertainty principle bound on a massless particle confined to a radius  $R \sim 1$  fm of  $E = p \gtrsim \sqrt{3}/R \simeq 342$  MeV (cf. Sect. XI-1). Model calculations have tended to use a somewhat larger effective gluon 'mass'.

<sup>9</sup> However, it should be understood that such a concept has not been shown to follow rigorously from  $QCD$ , nor indeed is a configuration of definite numbers of constituent gluons a gauge-invariant entity (cf. Sect. X-2).

Table XIII-3. Gauge-invariant color-singlet interpolating fields.

Operator	Dimension	$J^{PC}$
$\bar{q}\Gamma q$	3	$0^{-+}, 1^{-+}, 0^{++}, 1^{+-}, 1^{++}$
$\bar{q}\Gamma\mathcal{D}q$	4	$2^{++}, 2^{-\pm}$
$FF$	4	$0^{++}, 2^{++}, 0^{-+}, 2^{-+}$
$\bar{q}\Gamma qF$	5	$0^{\pm+}, 0^{\pm-}, 1^{\pm+}, 1^{\pm-}, 2^{\pm+}, 2^{\pm-}$
$F\mathcal{D}F$	5	$1^{++}, 3^{++}$

The basic idea of confinement is that only color-singlet states exist as physical hadrons. If we identify those states which are color singlets and which contain few quark or gluon quanta, we can easily find other possible configurations besides  $Q\bar{Q}$  and  $Q^3$ . Some of the more well-known examples are

- (1) Gluonia (or glueballs) – quarkless  $G^2$  or  $G^3$  states, which we shall discuss in more detail below,
- (2) Hybrids – color-singlet mixtures of constituent quarks and gluons like  $Q\bar{Q}G$  mesons or  $Q^3G$  baryons,
- (3) Dibaryons – six-quark configurations in which the quarks have *similar* spatial wavefunctions rather than two separate three-quark clusters,
- (4) Meson molecules – loosely bound deuteron-like composites of mesons.
- (5) Tetraquark states – strongly bound states with quark structures  $qq\bar{q}\bar{q}$ .

A convenient framework for describing the quantum numbers of possible hadronic states is obtained by considering gauge-invariant, color-singlet operators of low dimension [JaJR 86], as was discussed in Sect. XI-1. Table XIII-3 lists all such operators up to dimension five which can be constructed from quark fields,  $QCD$  covariant derivatives, and the gluon field strength, denoted respectively by  $q$ ,  $\mathcal{D}q$ ,  $\mathcal{D}F$ , and  $F$ . Also appearing in Table XIII-3 is the collection of  $J^{PC}$  quantum numbers associated with each such operator. Particular spin-parity values are obtained from these operators by choosing indices in appropriate combinations.

### *The first resonance – $\sigma(440)$*

The lightest resonance encountered in the meson spectrum has long been one of the most controversial states. This state is officially known as  $f_0(500)$ , but it is almost universally referred to as  $\sigma$ . The existence of this resonance has finally been established unambiguously. However, the interpretation remains remarkably subtle.

The scattering of two pions in the  $I = 0$  and  $J = 0$  channel becomes strong at low energies. The amplitude is described by chiral perturbation theory, as described in Sect. VII–3. At first order in the energy expansion, the scattering amplitude is<sup>10</sup>

$$T_{00}^{(0)} \equiv t_0 = \frac{s}{16\pi F_\pi^2}. \quad (4.1)$$

This amplitude is purely real, while under the general principle of unitarity of the  $S$  matrix the elastic amplitude must have the form

$$T_{00} = e^{i\delta_{00}} \sin \delta_{00}, \quad (4.2)$$

and has to satisfy

$$\text{Im } T_{00} = |T_{00}|^2. \quad (4.3)$$

The lowest-order amplitude of Eq. (4.1) has no imaginary part. However, in chiral perturbation theory, the imaginary part starts at order  $E^4$ , and the first contribution to this appears through one-loop diagrams. Chiral perturbation theory satisfies unitarity order by order in the energy expansion.

The  $\sigma$  appears as a resonance when exact unitarity is applied to the scattering amplitude. The pole can be seen in an exceptionally simple approximation. If one simply iterates the lowest-order amplitude one can produce a fully unitary result

$$T_{00} = \frac{t_0}{1 - it_0}, \quad (4.4)$$

which satisfies Eq. (4.3) exactly and also reproduces the chiral result to first order. The use of Eq. (4.1) with a complex value for  $s$  as the input for Eq. (4.4) produces a pole on the second sheet at

$$\sqrt{s} = (1 - i)\sqrt{8\pi}F_\pi = (460 - i460) \text{ MeV}. \quad (4.5)$$

This is the first approximation to the  $\sigma$ .

The complete analysis is much more subtle, but carries a similar result. By including not only unitarity, but also crossing symmetry and analyticity, one can obtain a dispersive representation of the scattering amplitude [Ro 71]. When evaluated using chiral constraints at low energy and data at high energy, the  $\pi\pi$  data can be fully described [CoGL 01]. When extended into the complex plane, the real  $\sigma$  pole appears at [CaCL 06]

$$\sqrt{s} = m_\sigma - i\frac{\Gamma_\sigma}{2} = (441 - i272) \text{ MeV}. \quad (4.6)$$

<sup>10</sup> In order to keep the formulas simple and physically transparent in this introductory section, we present them with the pion mass set equal to zero.

However, this does not appear as a typical resonance. In contrast to others, the  $\sigma$  width is larger than its mass, indicating that the pole is far from the physical values of  $s$ . Moreover, in the scattering amplitude itself, there is no sign of a resonant bump. The phase shift rises almost linearly from  $\delta_{00} = 0$  at threshold to  $\delta_{00} = 100^\circ$  around 900 MeV. The phase shift does go through  $90^\circ$ , traditionally a sign of a resonance in elastic scattering, but at an energy  $\sqrt{s} \sim 850$  MeV which is far removed from the pole position. These unusual features had long created confusion about the existence of the  $\sigma$ , which has been cleared up only through the rigorous combination of chiral and dispersive techniques.

The  $\sigma$  is a dynamical strong-coupling resonance. The resonance does not fit naturally into the quark model and it does not seem profitable to try to force the  $\sigma$  into that framework. While we do expect to see quark model bound states as resonances, there is no requirement that all resonant behavior must be associated with quark model states. Indeed, there is a strong theoretical argument that the  $\sigma$  is different from the bound states of  $QCD$  [Pe 04]. Recall two features of the large  $N_c$  limit discussed in Chap. X – that the meson bound states stay constant in mass when the large  $N_c$  limit is taken, but scattering amplitudes fall like  $1/N_c$ . This latter requirement is satisfied for the  $\pi\pi$  amplitudes; in the lowest-order amplitude of Eq. (4.1), the amplitude falls with  $N_c$  because  $F_\pi \sim \sqrt{N_c}$  appears squared in the denominator. Because the  $\pi\pi$  amplitude is smaller at larger  $N_c$ , the amplitude becomes of order unity at a higher energy. If the  $\sigma$  is indeed connected with the strong coupling of  $\pi\pi$  scattering, its mass will shift to higher energy as  $N_c$  increases. While we cannot change  $N_c$  in the scattering data themselves, there are straightforward analytic methods, such as the inverse-amplitude method [DoP 97], which is a variant of Padé techniques,<sup>11</sup> to closely describe the data including chiral perturbation theory and exact unitarity. Use of such techniques is able to reproduce the  $\sigma$  found in the data, and then when  $N_c$  is varied one finds [Pe 04],

$$m_\sigma \sim \sqrt{N_c}, \quad (4.7)$$

as expected by the general argument. Indeed, even our simplified approximation of Eq. (4.5) has this behavior, again due to  $F_\pi \sim \sqrt{N_c}$ . Because the bound states of  $QCD$  should behave as a constant,  $m \sim N_c^0$ , the  $\sigma$  appears distinct from these. It appears to be a resonance associated with the unitarity of elastic scattering.<sup>12</sup>

Some caveats and cautions about this result are appropriate. This experimental resonance does not appear to be the  $\sigma$  of the linear  $\sigma$  model. As described in Chaps. IV and VII, the coefficients of the chiral lagrangian are sensitive to the underlying fundamental theory, and the coefficients found for  $QCD$  do not resem-

<sup>11</sup> Our approximation of Eq. (4.5) above is equivalent to the lowest order of the inverse amplitude method.

<sup>12</sup> Other states that may have a related origin include the  $\kappa(800)$  seen in  $K\pi$  scattering and the  $N(1405)$  in  $\pi N$  scattering.

ble those of the linear  $\sigma$  model. Nor is the existence of this state a justification to use a fundamental  $\sigma$  field in field-theoretic calculations. While the use of  $\sigma$  exchange with a particular coupling may be a proxy for  $\pi\pi$  effects in a given reaction, this use is not necessarily valid in general. The use of a fundamental  $\sigma$  is much more restrictive than the variety of pionic effects. Moreover, it is neither an accurate nor controlled approximation, and may double-count the pionic contributions, which must also be included.

In addition, the above discussion provides a cautionary counterexample to a widely used argument. It is common to use the violation of tree unitarity of an effective theory as an indication of the energy at which New Physics should be seen [LeQT 77], with the expectation that the New Physics would restore unitarity. In the situation discussed above, the usual measure of tree-unitarity violation,  $\text{Re } T_{00} \leq 1/2$ , occurs at 460 MeV, which is well below the production threshold of the quarks and gluons of  $QCD$ . Also, the energy of tree-unitarity violation varies as  $\sqrt{N_c}$  in units where the scale of  $QCD$  is held fixed [AyAD 12]. Thus, any ‘New Physics’ does not have the same  $N_c$  scaling. The strongly coupled effective theory manages to respect unitarity without new degrees of freedom. The situation above indicates that, while the violation of tree unitarity does indicate the existence of a strongly coupled region, its use as an indicator of New Physics must be treated with caution.

### *Gluonia*

The existence of a gluon degree of freedom in hadrons is beyond dispute, with evidence from deep-inelastic lepton scattering and jet structure in hadron–hadron collisions. However, trying to predict the properties of a new class of hadrons whose primary ingredient is gluonic is nontrivial. Hypothetically, if quarks could be removed from  $QCD$  the resulting hadron spectrum would consist only of *gluonia* (or ‘glueballs’).

Gluonic configurations should be signaled by the existence of extra states beyond the expected nonets of  $Q\bar{Q}$  hadrons. However, mixing with  $Q\bar{Q}$  hadrons is generally possible (cf. Sect. X–2). Although predicted by the  $1/N_c$  expansion to be suppressed, such mixing effects serve to cloud the interpretation of data vis-à-vis gluonium states. Referring to the interpolating fields mentioned above, we see that for gluons the gauge-invariant combinations

$$F_{\mu\nu}^a F^{a\mu\nu}, \quad F_{\mu\lambda}^a F_{a\nu}^\lambda, \quad F_{\mu\nu}^a \tilde{F}^{a\mu\nu}, \quad F_{\mu\lambda}^a \tilde{F}_{a\nu}^\lambda \quad (4.8)$$

can be formed out of *two* factors of a gluon field-strength tensor  $F_{\mu\nu}^a$  or its dual  $\tilde{F}^{a\mu\nu}$ . The spin, parity, and charge conjugation carried by these these operators are respectively  $J^{PC} = 0^{++}, 2^{++}, 0^{-+}, 2^{-+}$ , and are thus the quantum numbers

expected for the lightest glueballs,<sup>13</sup> i.e., such operators acting on the vacuum state produce states with these quantum numbers. Although there is no *a priori* guarantee that one obtains a single particle state (e.g., a  $2^{++}$  operator could in principle create two  $0^{++}$  glueballs in a  $D$  wave), the simplicity of the operators leads one to suspect that this will be the case. There is one, somewhat controversial, construct missing from the above list. Two massive spin-one particles in an  $S$  wave can have  $J^{PC} = 1^{-+}$  as well as  $J^{PC} = 0^{++}, 2^{++}$ , and some models predict such a gluonium state. However, a  $1^{-+}$  combination of two massless on-shell vector particles is forbidden by a combination of gauge invariance plus rotational symmetry [Ya 50]. The lack of a  $1^{-+}$  gauge-invariant, two-field operator is an indication of this.

Aside from a list of quantum numbers and some guidance as to relative mass values, theory does not provide a very clear profile of gluonium phenomenology. Lattice-gauge methods offer the best hope for future progress. Present quenched lattice studies predict that in a quarkless version of  $QCD$  the lightest glueball is a  $0^{++}$  state of mass  $1.7 \pm 0.1$  GeV and while the  $2^{++}$  and  $0^{-+}$  glueballs are about  $1.4 \pm 0.1$  times heavier [Ba *et al.* 93], [MoP 99], [Ch *et al.* 06].

The challenge arises when couplings to quark degrees of freedom are introduced, in which case substantial mixing between quark and gluonium states must occur. Lattice studies of the mixing with the  $0^{++}$  state have yielded mixed results, some indicating a lowering of the mass by as much as several hundred MeV [Ha *et al.* 06], while others show little effect [Ri *et al.* 10]. It is generally agreed that inclusion of quarks has little effect on the mass of the  $2^{++}$  and  $0^{-+}$  states [Ri *et al.* 10], [HaT 02]. The problem has also been studied via  $QCD$  sum rules with inclusion of instanton effects, but again there exists considerable uncertainty [Fo 05], [Ha *et al.* 11].

Gluonium states would be classified as flavor- $SU(3)$  singlets and if mixing with quark states exist there should exist ‘extra’ such states. An example of this phenomenon exists in the 1.5 GeV region where the states

$$f_0(1370), f_0(1500), f_0(1710), K_0^*(1430), a_0(1450)$$

can be interpreted as a nonet of  $q\bar{q}$  states plus a glueball [AmC 96]. In this picture the three  $f_0$  states are mixtures of the  $0^{++}$  glueball and the two  $q\bar{q}$  states from the nonet. The validity of this description relies on the existence of these three  $f_0$  resonances. While the  $f_0(1500)$  and  $f_0(1710)$  are reasonably well established and have significant two-meson decay channels, the same is not true of the  $f_0(1370)$ , which, if it does exist, has a large (>80%) decay fraction into  $4\pi$ . For this reason the interpretation in terms of three-channel mixing of these states is still

<sup>13</sup> Gluonic operators with *three* field-strength tensors produce states with  $J^{PC} = 0^{\pm+}, 1^{\pm+}, 2^{\pm+}, 1^{\pm-}, 2^{\pm-}, 3^{\pm-}$ . Because of the extra gluon field, one expects these states to be somewhat heavier.

Table XIII–4. Spectroscopy of six-quark configurations.

$SU(6)$ of color-spin	$SU(3)$ of flavor	Spin
490	1	0
896	8	1,2
280	10	1
175	10*	1,3
189	27	0,2
35	35	1
1	28	0

controversial. Thus, despite 30 years of work on the problem of glueballs, the situation remains confused. A recent review of the subject can be found in [Oc 13].

#### *Additional nonconventional states*

There is a widespread belief that gluonium states *must* appear in the spectrum of the *QCD* hamiltonian, though as discussed above it has proved challenging to identify them. For other kinds of nonconventional configurations, it is also difficult to reach a meaningful consensus, although experimental efforts to detect such states are ongoing. We briefly review several such possibilities.

(i) *Hybrids*: From Table XIII–3, we see that among the  $\bar{Q}QG$  meson hybrids is one with the quantum numbers  $J^{PC} = 1^{-+}$ . This would-be hadron is of particular interest because comparison with Table XI–3 reveals that it cannot be a  $\bar{Q}Q$  configuration. Model calculations suggest that the lightest such state should be isovector, with mass in the range 1.5–2.0 GeV, and that such states may largely decouple from  $L = 0$   $\bar{Q}Q$  meson final states. A study of  $Q^3G$  baryon hybrids reveals that *none* of the states is exotic in the sense of lying outside the usual  $Q^3$  spectrum [GoHK 83].

(ii) *Dibaryons*: The most remarkable aspect learned yet about the dibaryon states is how much six-quark configurations are restricted by Fermi–Dirac statistics. Table XIII–4 lists the possible six-quark  $SU(3)$  multiplets along with their spin values [Ja 77]. Of this collection of states, the most attention has been given to the spinless  $SU(3)$ -singlet state, called the *H-dibaryon*. This particle, which has strangeness  $S = -2$  and isospin  $I = 0$ , is predicted to be the lightest dibaryon, and if bound would be unstable to weak decay. A series of experiments has failed to find the H, so at this time there is no evidence for the existence of dibaryons.

(iii) *Hadronic molecules and tetraquarks*: Particles with the quark content  $qq\bar{q}\bar{q}$  also form color singlets. The literature distinguishes two types of such states:

hadronic molecules and tetraquarks. Roughly speaking, the molecular states refer to two separate  $q\bar{q}$  color-singlet states that are lightly bound. Since the binding energy is small, such states could be expected to be found right near the threshold for the two mesons. Tetraquarks refer to configurations where the  $qq\bar{q}\bar{q}$  constituents are more compactly intertwined, with the details of the configuration varying in different models. Clearly, there can be a continuum interpolating between these extremes. We will not enter into the debate about the signals for the two classes of four-quark states.

There appears to be clear evidence for the existence of a state in this category. The  $Z_c(3900)$  [Li *et al.* 13] [Ab *et al.* 13] has mass and production properties that indicate that it contains a  $c\bar{c}$  pair. However, it also carries a charge which proves that it also contains light quarks with the  $u\bar{d}$  combination producing the positive charge. The internal configuration has not been sorted out yet.

Among the particles that have been discussed as molecules are the isovector  $a_0(980)$  and isoscalar  $f_0(975)$  mesons. Nominally, these particles have the quantum numbers of the  $L = 1$  sector of the  $Q\bar{Q}$  model, and their near equality in mass suggests an internal composition similar to that of the  $\rho(770)$  and  $\omega(783)$ , i.e., orthogonal configurations of nonstrange quark–antiquark pairs. However, among properties which argue against this are their relatively strong coupling to modes which contain strange quarks, their narrower-than-expected widths, and their  $\gamma\gamma$  couplings. The proximity of the  $K\bar{K}$  threshold and the importance of the  $K\bar{K}$  modes has motivated their interpretation as  $K\bar{K}$  molecules [Wei 83]. However, interpretation of scattering data near the 1 GeV region is not clear, and indeed a strong case has been made for the alternative  $qq\bar{q}\bar{q}$  picture [’tHooftIMPR 08] and for heavier states as well.

A clearer situation is provided by the  $X(3872)$ , which has been interpreted in terms of a  $D_0-\bar{D}_0^*$  hadronic molecule, which is bound by  $\pi^0$  exchange at long distance and quark/color exchange at short distances. That  $X(3872)$  is not a simple charmonium state is indicated by large isospin violation seen in the data. This occurs in the molecule interpretation because the mass of the resonance is essentially identical to  $m_{D_0} + m_{D_0^*}$  and considerably lighter than  $m_{D^+} + m_{D^{*-}}$ . Thus, the molecular state would predominantly involve  $D_0-\bar{D}_0^*$  containing  $c\bar{c}u\bar{u}$  quarks, so that this structure is a mixture of isospin states

$$c\bar{c}u\bar{u} = c\bar{c}\sqrt{\frac{1}{2}} \left[ \sqrt{\frac{1}{2}}(u\bar{u} + d\bar{d}) + \sqrt{\frac{1}{2}}(u\bar{u} - d\bar{d}) \right] \quad (4.9)$$

In this picture there should be nearly comparable decays to final states with  $I = 0$  and  $I = 1$ , and this is indeed indicated by significant branching ratios of the  $X(3872)$  to both  $J/\psi\rho$  and  $J/\psi\omega$  modes.

Other examples of four-quark states may occur in the  $b\bar{b}$  system and the resonances  $X_b^+(10610)$  and  $X_b^+(10650)$ , which appear to be a bound states of  $B^+-\bar{B}^{0*}$  and  $B^{0*}-\bar{B}^{+*}$ , respectively. In this case the states are charged, with quark content  $b\bar{b}u\bar{d}$ , so that both states are clearly exotic—they cannot be excited bottomonium.

The overall interpretation of these states is complicated by the fact that molecules and tetraquarks have the same quark content and are distinguished only by details of their internal configuration. In some cases, both interpretations have advocates [AIHW 12, Du *et al.* 10].

## Problems

### (1) Power-law potential in quarkonium

Consider an interquark potential of the form  $V(r) = cr^d$ .

- Use the virial theorem to determine  $\langle T \rangle / \langle V \rangle$  for the ground state.
- Given the form  $E_{2S} - E_{1S} = f(d)M^{-d/(2+d)}$ , where  $M$  is the reduced mass, determine  $d$  from the observed mass differences in the  $c\bar{c}$  and  $b\bar{b}$  systems, using Eq. (3.1) to supply heavy-quark mass values.
- Assuming this model is used to fit the spin-averaged ground-state  $c\bar{c}$  and  $b\bar{b}$  mass values, determine  $v^2/c^2$  for each system.

### (2) Quarkonium annihilation from the $^1S_0$ state

Modify Eq. (1.15) to obtain the leading-order contributions appearing in Eq. (1.16).

### (3) Mass relations involving heavy quarks

- Repeat the analysis of Eq. (3.1) but using the masses of the charmed/strange mesons  $D_s, D_s^*$  instead. Infer a value for  $\hat{M}/M_c$  by referring to the result obtained in Eq. (2.17). Compare with the determination of Eq. (3.1).
- Extend the procedure of Eqs. (2.20–2.25) to isospin-violating mass differences of  $c$ -flavored and  $b$ -flavored hadrons.